Available online at www.sciencedirect.com

ScienceDirect

Procedia Engineering 116 (2015) 818 – 823

Procedia Engineering

www.elsevier.com/locate/procedia

8th International Conference on Asian and Pacific Coasts (APAC 2015)

Algorithm for Detection of Current and Water-depth using X-band Marine Radar

Kyungmo Ahn[a]*, Chan Young Oh[a], Hwusub Chun[b]

[a]*Handong Global University, 3 Namsong-ri, Heunghae, Pohang City 791-708, Korea*
[b]*Samsung Electronics, 1 samsungjeonja-ro, Hwaseong-si, Gyeonggi-do, 445-701, Korea*

Abstract

The object of this study is to present an algorithm to estimate ambient current and water depth from sea clutter images obtained from X-band marine radar. In the present article, numerically synthetized images are utilized to verify the accuracy of the proposed algorithm. Synthetized sea surface images were analyzed for regular directional waves as well as directional random waves with current and without current. Estimation of currents from sea surface images for cases of known water depth showed good agreement with exact current velocity. However, we have some computational difficulty when prior water depth is unknown.

Peer- Review under responsibility of organizing committee , IIT Madras , and International Steering Committee of APAC 2015

Keywords: X-band radar; random waves; current velicity; sea surface image

1. Introduction

In recent years, it has been demonstrated that radar images of the ocean surface provide reliable information on the spatial behavior of wave fields. Many systems which utilize a commercial marine X-band radar for providing time series of radar backscatter images from the sea surface have been developed. (Borge et al., 2004, Plant and Zunk, 1997) Wave measurement system using marine X-band radar has many advantages over conventional wave gages, which is more robust in severe sea state, easy to maintain, cheap maintenance cost, etc.

* Corresponding author. Tel.: +82-10-2815-8661; fax: +82-54-260-1429.
E-mail address: kmahn@handong.edu

Peer- Review under responsibility of organizing committee , IIT Madras , and International Steering Committee of APAC 2015
doi:10.1016/j.proeng.2015.08.369

However, one critical shortcoming of X-band radar system for operational wave measurements exists which is it's inaccuracy in the estimation of wave heights during weak local wind conditions. It is not an easy task to overcome this critical shortcoming. It is because this problem resides in the X-band radar system's inherent sea surface scanning mechanism called Bragg Resonance mechanism.

For the case of X-band radar (frequency of 9.4 GHz), sea surface with ripple waves (wavelength of about 2 cm) provide Bragg resonance, henceforth make it possible to estimate reliable wave heights. On the other hand, swell waves without ripples during no local wind condition, are tend to be significantly underestimated. It is because the backscattered radar signals from smooth sea surface without ripples result in weak scattered image intensity. However, this critical shortcomings of X-band radar system could be calibrated by considering peak wave frequency information for the fully developed swell waves. (Ahn et al., 2014)

Fig. 1 shows an example of sea clutter image obtained from X-band marine radar system. The polar image in the figure shows the waves approaching to the coastline from the north-eastern direction. Cartesian image within red box with a size of 600m by 600m is used to obtain the wave and the mean current information.

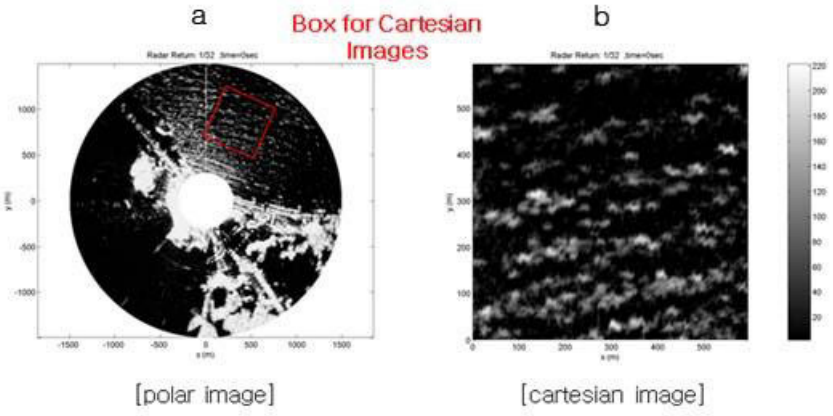

Fig. 1. (a) Example of sea clutter image obtained from X-band marine radar; (b) Cartesian image for the analysis of waves and current.

The objective of the paper is to propose an algorithm to estimate current and water depth using sea clutter images obtained from X-band marine radar system. Synthesized sea surface images were used to verify the accuracy of the algorithm.

2. Algorithm

Based on the linear wave theory, the dispersion equation with ambient currents can be written as

$$\omega = \vec{k} \cdot \vec{U} + \sqrt{gk \tanh kh} \qquad (1)$$

where ω: radian frequency, $\vec{k}$: wave number vector, $|\vec{k}| = k$, $\vec{U}$: current velocity, g: gravitational acceleration, h: water depth. For a given water depth, the shapes of the dispersion equation written in Eq. (1) can be drawn with and without current available as shown below:

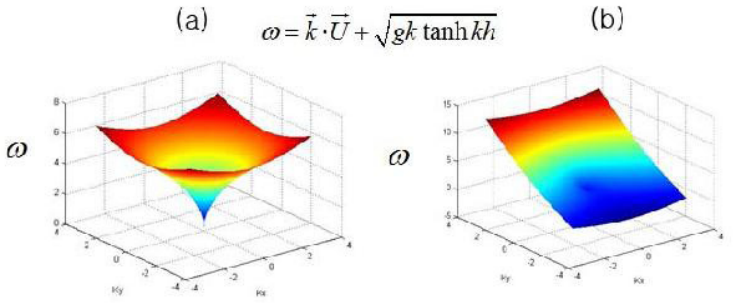

Fig. 2. Dispersion shell of $\omega = \vec{k} \cdot \vec{U} + \sqrt{gk \tanh kh}$ (a) without current; (b) with current, respectively.

From Eq.(1), the current velocity $\vec{U} = (u_x, u_y)$ is to be determined. The following functional should be minimized in order to estimate the current vector and water depth.

$$Q^2 = \sum_{j=1}^{N} (\omega_j - k_{xj} u_x - k_{yj} u_y - \sigma)^2 \tag{2}$$

where $\sigma = \sqrt{gk \tanh kh}$ is intrinsic frequency.

In order to have a minimum functional for unknowns u_x, u_y and *h*, the following conditions can be used

$$\frac{\partial Q^2}{\partial x} = 0, \quad \frac{\partial Q^2}{\partial y} = 0, \quad \frac{\partial Q^2}{\partial h} = 0 \tag{3}$$

From equations (2) and (3), we get

$$U_x \left(\sum_{j=1}^{N} k_{xj}^2 \right) + U_y \left(\sum_{j=1}^{N} k_{xj} k_{yj} \right) - \sum_{j=1}^{N} (\omega_j - \sigma_j) k_{xj} = 0 \tag{4}$$

$$U_x \left(\sum_{j=1}^{N} k_{xj} k_{yj} \right) + U_y \left(\sum_{j=1}^{N} k_{yj}^2 \right) - \sum_{j=1}^{N} (\omega_j - \sigma_j) k_{yj} = 0 \tag{5}$$

$$\sum_{j=1}^{N} (\omega_j - k_{xj} U_x - k_{yj} U_y - \sigma_j) \cdot \frac{gk^2 (1 - (\tanh kh)^2)}{\sigma_j} = 0 \tag{6}$$

Eqs. (4), (5) and (6) can be solved simultaneously to get unknown u_x, u_y and *h*.

3. Verification of the Algorithm

In order to verify the proposed algorithm, we numerically synthetized sea surface images with current and without current. First, we start to solve Eqs. (4) and (5) for assumed water depth (maybe initial water depth assumed to be deep water) . Then, we plugging u_x, u_y and *h* values in Eq.(6) to see whether Eq. (6) is satisfied or not. If not, go back to solve Eq. (4) and (5) with decreased water depth until Eq. (6) is satisfied.

3.1 Regular wave cases

We start with wave equation with single component as follows:

$$\eta = \frac{3}{2} \cos(k_x x + \omega t) + 2 \cos(k_x x + \omega t + \phi) \tag{7}$$

Fig.(3) shows single frequency wave propagation with and without current velocity. The estimated current speed obtained from sea surface image shows good agreement with the exact speed as shown in the figure.

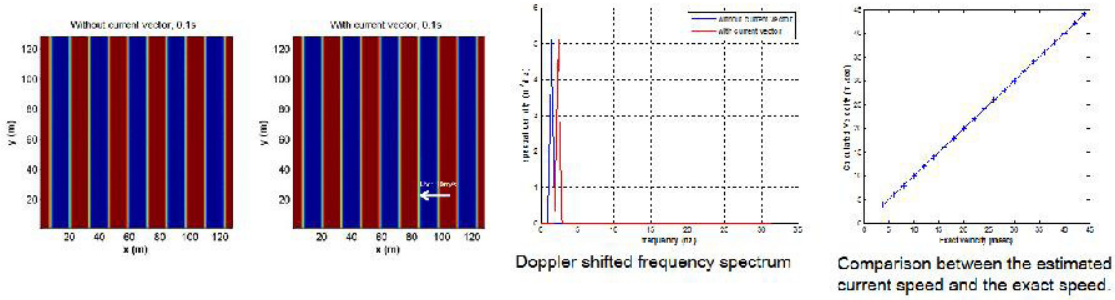

Fig. 3. Plan view of wave propagation with and without current, respectively. Doppler shifted frequency spectrum and comparison between the estimated current speed and the exact speed.

The second numerical test cases were conducted with two wave components propagating in different directions. Wave equation tested is as follows:

$$\eta = \cos(k_{1x}x + k_{1y}y - \omega_1 t) + 2\cos(k_{2x}x + k_{2y}y - \omega_2 t + \phi) \tag{8}$$

Fig.4 shows two wave components are propagation with and without current cases. The estimated current direction and speed showed good agreement with the exact ones as shown in the figure.

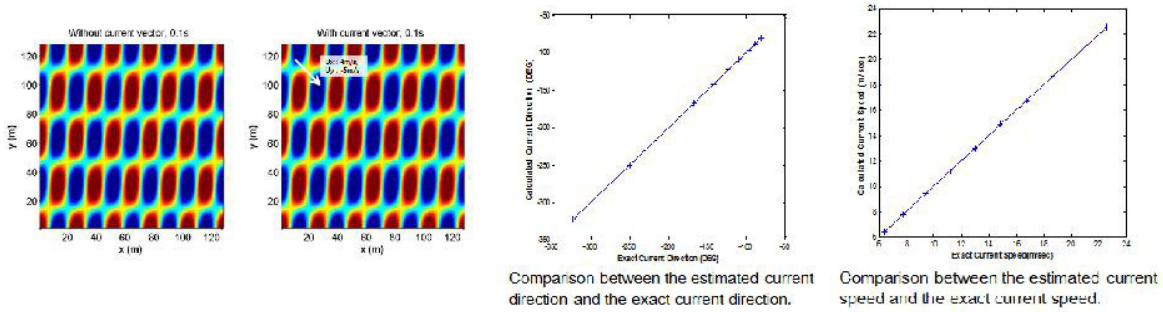

Fig. 4. Plan view of wave propagation with and without current, respectively. Comparison between the estimated current direction and the exact current direction. Comparison between the estimated speed and the exact speed.

3.2 Random wave cases

For the random wave test case, we analyzed synthetized random waves using directional spectrum, $S(f,\theta)$, with JONSWAP frequency spectrum and Mitsuyasu spreading function.

$$S(f,\theta) = S(f)\cdot D(f,\theta)$$

The parameters in JONSWAP spectrum are

$$S(f) = \beta_J H_s^2 T_p^{-4} f^{-5} \exp\left[-1.25\left(T_p f\right)^{-4}\right]\gamma^{\exp\left(-\left(T_p f-1\right)^2/2\sigma^2\right)}$$

where $\gamma = 3.3$ and

$$\beta_J = \frac{0.0624\left(1.094 - 0.01915\log\gamma\right)}{0.230 + 0.0336\lambda - 0.185\left(1.9+\gamma\right)^{-1}},\ \sigma = \begin{cases} 0.07 & f \le f_p \\ 0.09 & f > f_p \end{cases}$$

and the Mitsuyasu spreading function is

$$D(\theta, f) = \frac{2^{2s-1}}{\pi}\frac{\left\{\Gamma(s+1)\right\}^2}{\Gamma(2s+1)}\left|\cos\left(\frac{\theta}{2}\right)\right|^{2s}$$

where $s_{\max} = 2.5,\ s = \begin{cases} s_{\max}\left(f/f_p\right)^5 & f \le f_p \\ s_{\max}\left(f/f_p\right)^{-2.5} & f > f_p \end{cases}$

Fig. 5 shows the numerically synthetized sea surface with significant wave height, $H_s = 4m$, peak period, $T_p = 8.53s$, and mean wave direction, $\theta = 45^\circ$. Current vectors were generated by using following formula.

$$u_x = \cos\left(\frac{pi}{8}(j\text{-}1)\right),\ u_y = \sin\left(\frac{pi}{8}(j\text{-}1)\right)$$

where $j = 1, 2, ..., 16$

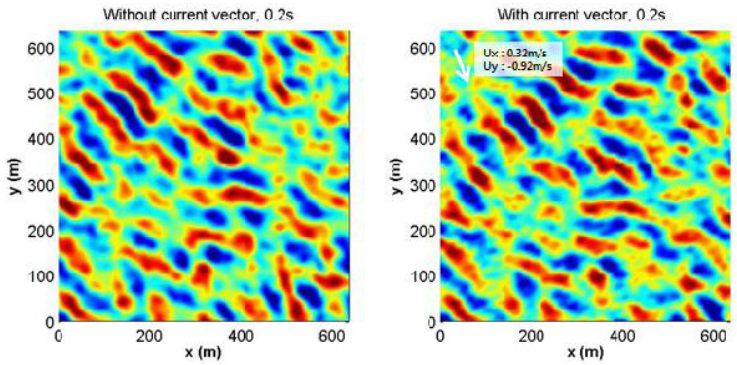

Fig. 5. Synthetized random sea surface without current and with current

Fig. 6 shows the comparison of estimated current velocities in x-direction and y-direction with exact velocities, respectively. Even for directional random seas, we could estimate the ambient current velocities, u_x and u_y with correlation coefficients of 0.965 and 0.962, respectively. Wave number spectra obtained from sea surface images with current and without current are shown in Fig. 7.

Estimation of water depth together with current velocity involves convergence in iteration process. We have some computational difficulty in solving Eq. (4), (5), and (6), simultaneously. We hope to present the results in the conference. The proposed algorithm has been implemented in X-band wave measurement system called 3S-System. More detailed analysis on the estimation of currents including rip current will be discussed more in the conference.

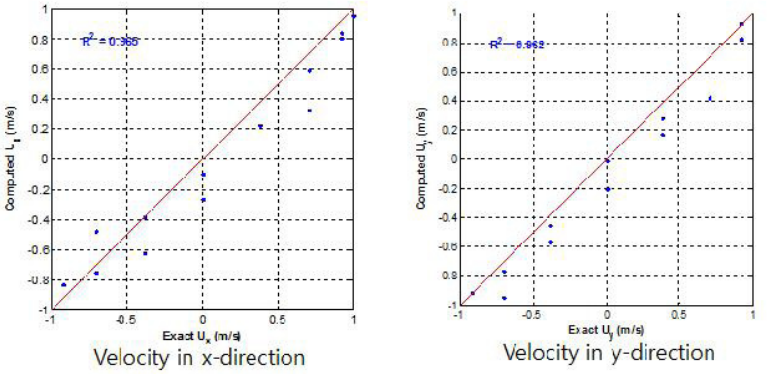

Fig. 6. Comparison of estimated current velocities in x-direction and y-direction with exact velocities.

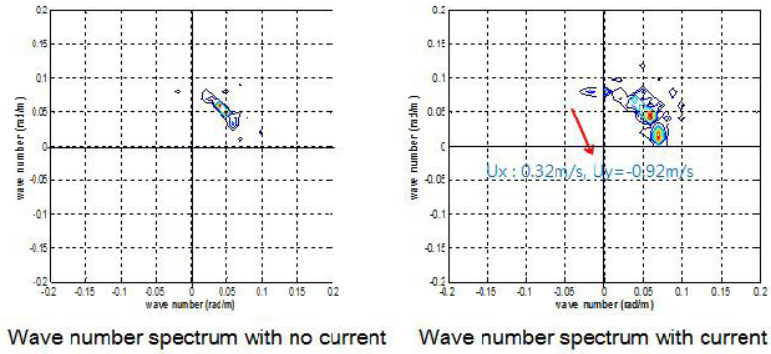

Fig. 7. Wave number spectra without current and with current.

Acknowledgements

This study was performed by projects of ‘Investigation of large swell waves and rip currents and development of the disaster response system (No. 20140057)’ and ‘Gyeonbuk Sea Grant Program’ sponsored by the Ministry of Oceans and Fisheries.

References

Borge, J.C.N., Rodriguez, K., Hessner, P.I., Gonzalez, P.I., 2004. Inversion of marine radar images for surface wave analysis, American Meteorological Society, 21, 1291–1300.

Plant, W.J., Zunk, L.M., 1997. Dominant wave directions and significant wave heights from SAR imagery of the ocean, Jornal of Geophysical Research, , 21, 3473–3482.

Ahn, K., Chun, H., Cheon, S.H., 2014. New calibration method applicable to significant wave heights obtained by X-band radar, 34th International Conference on Coastal Engineering, Seoul, Korea.